Electronic Supplementary Information (ESI)

Robust Synthesis of Ultrathin Au-Ag Nanowires as a High-Surface-Area, Synergistic Substrate for Constructing Efficient Pt-Based Catalysts

Shumeng Zhang, Lei Zhang, Zhaojun Liu, Moxuan Liu, Qikui Fan, Kai Liu, and Chuanbo Gao*

Frontier Institute of Science and Technology and State Key Laboratory of Multiphase Flow in Power Engineering, Xi'an Jiaotong University, Xi'an, Shaanxi 710054, China.

**E-mail: gaochuanbo@mail.xjtu.edu.cn*

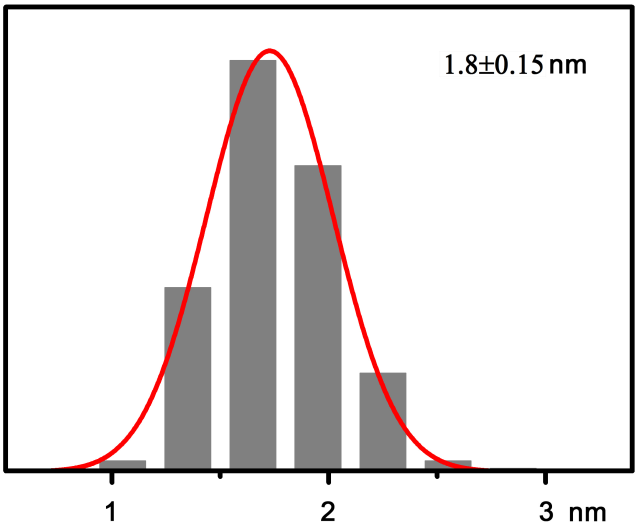

Figure S1. Diameter distribution of the ultrathin Au-Ag alloy nanowires obtained in a typical synthesis (TEM images see Figure 1). The average diameter is 1.8 nm, and the standard deviation is 0.15 nm.

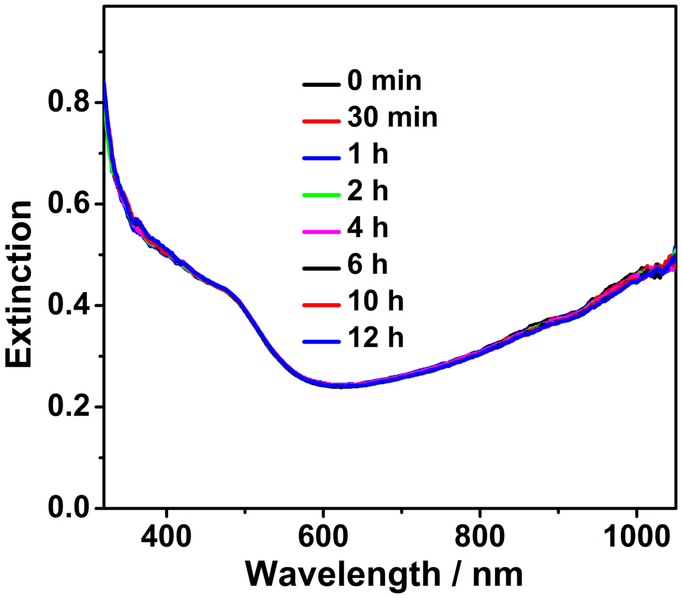

Figure S2. Stability of the ultrathin Au-Ag alloy nanowires against oxidative etching by H_2O_2 (1 M) in the presence of PVP. The ultrathin Au-Ag alloy nanowires showed no significant change in the UV-vis-NIR spectroscopy when exposed to the strong oxidizing agent for up to 12 h, which confirms that the nanowires are composed of an alloy of Au and Ag rather than individual segments of the metals.

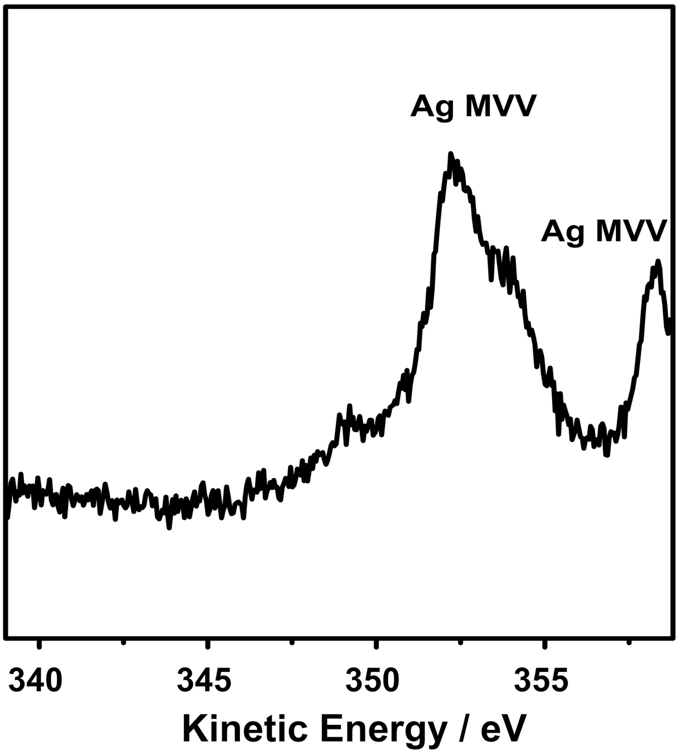

Figure S3. Auger electron spectroscopy of Ag in the ultrathin Au-Ag alloy nanowires. Two peaks can be observed at 352.2 and 358.4 eV of the kinetic energy, corresponding to the Ag(0). No peaks can be observed at 351.2 or 356.6 eV (corresponding to Ag(I) species). It confirms that Ag is present as elemental Ag(0) that is alloyed with Au in the nanowires.

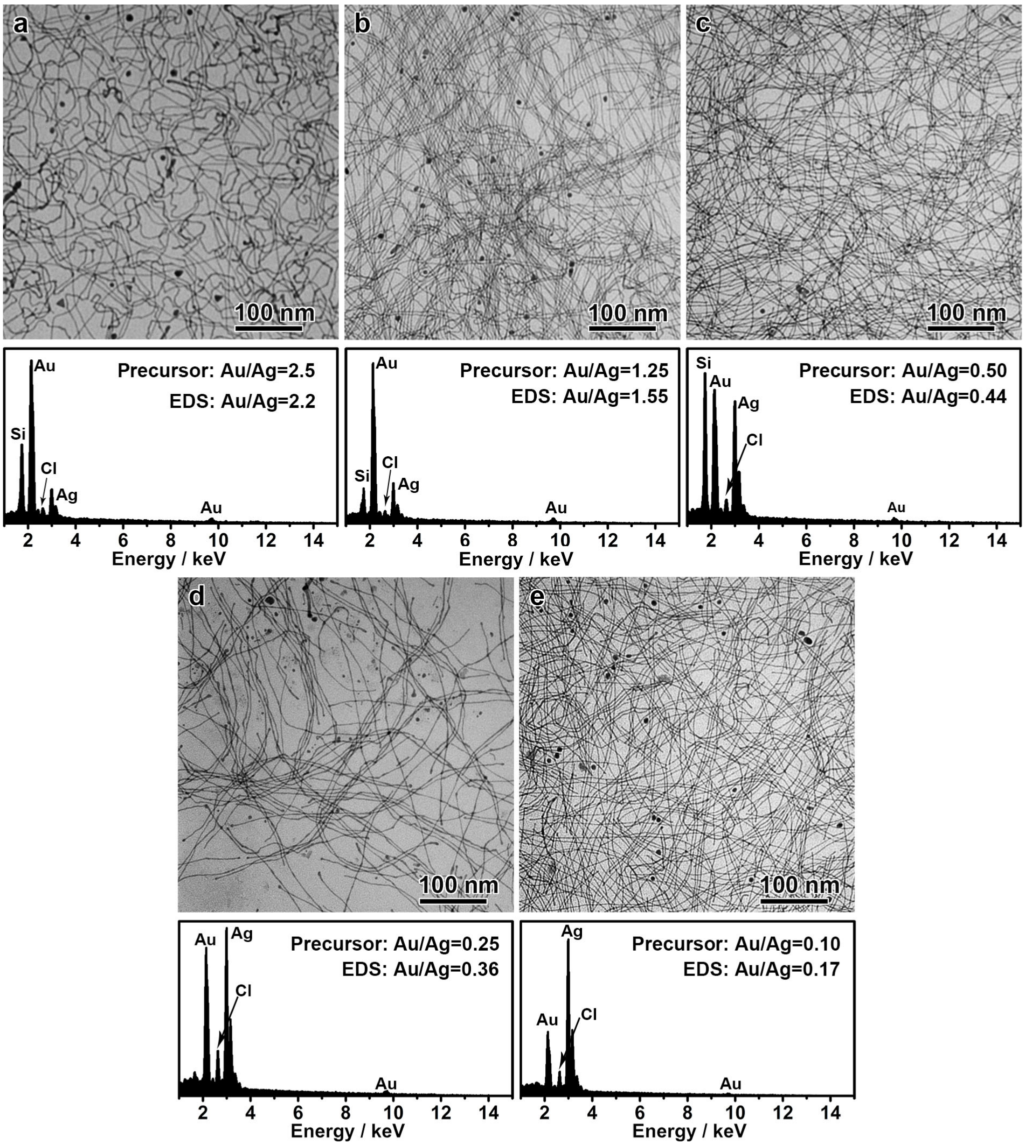

Figure S4. The tunability of the Au/Ag ratio in the ultrathin Au-Ag alloy nanowires. (a–e) TEM images and EDS spectra of the nanowires synthesized with $HAuCl_4/AgNO_3$ ratios of 2.5, 1.25, 0.50, 0.25, and 0.10, respectively, in the feeding precursors. It is worth noting that additional Cl^- was added in (c–e), resulting in a Cl^-/Ag^+ ratio of 10; otherwise, nano-tadpoles formed instead of nanowires. We can successfully synthesize ultrathin Au-Ag nanowires with a broad Au/Ag ratios of 2.2 to 0.17, as determined by the EDS, by adjusting the ratio of $HAuCl_4/AgNO_3$ in the feeding precursors. The Au/Ag ratio in the nanowires is in good agreement with the ratio of $HAuCl_4/AgNO_3$ in their precursors. The excellent control over the Au/Ag ratio confirms the high versatility of this synthesis strategy in producing ultrathin Au/Ag nanowires with varying properties.

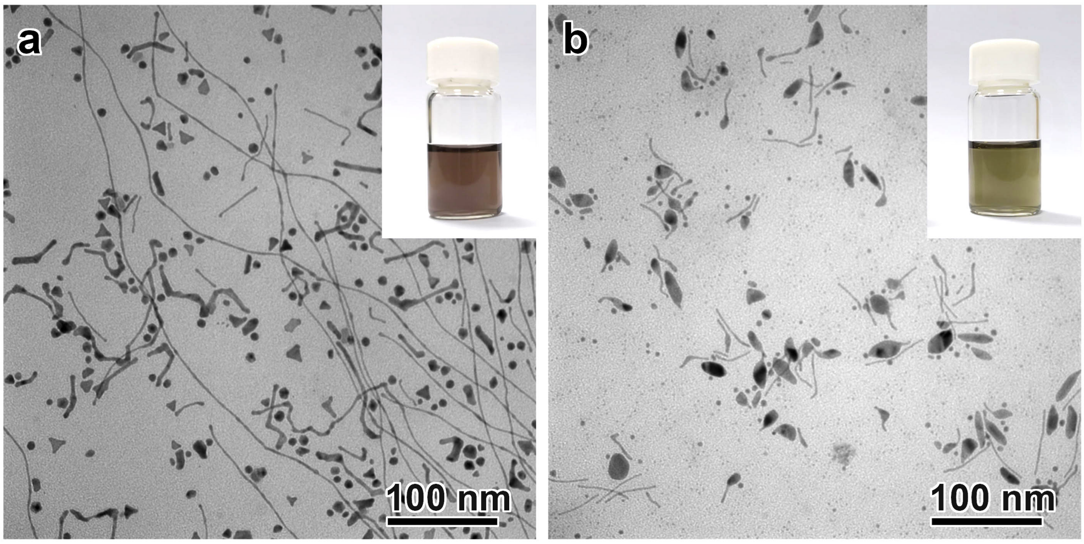

Figure S5. Synthesis of the ultrathin Au-Ag alloy nanowires with extremely high or low $HAuCl_4/AgNO_3$ ratios in the feeding precursor. (a) $HAuCl_4/AgNO_3 = 3$. (b) $HAuCl_4/AgNO_3 = 0.05$ (with Cl^-/Ag^+ ratio of 10). Inset: photographs of the product. In both cases, a mixture of nanoparticles and nanowires was obtained. Combined with Figure S4, it can be concluded that the Au/Ag ratio in the ultrathin Au-Ag alloy nanowires could be tuned in a range of 0.17–2.2 (determined by EDS); it is very difficult to synthesize ultrathin Au-Ag alloy nanowires with extreme Au/Ag ratios in a high yield.

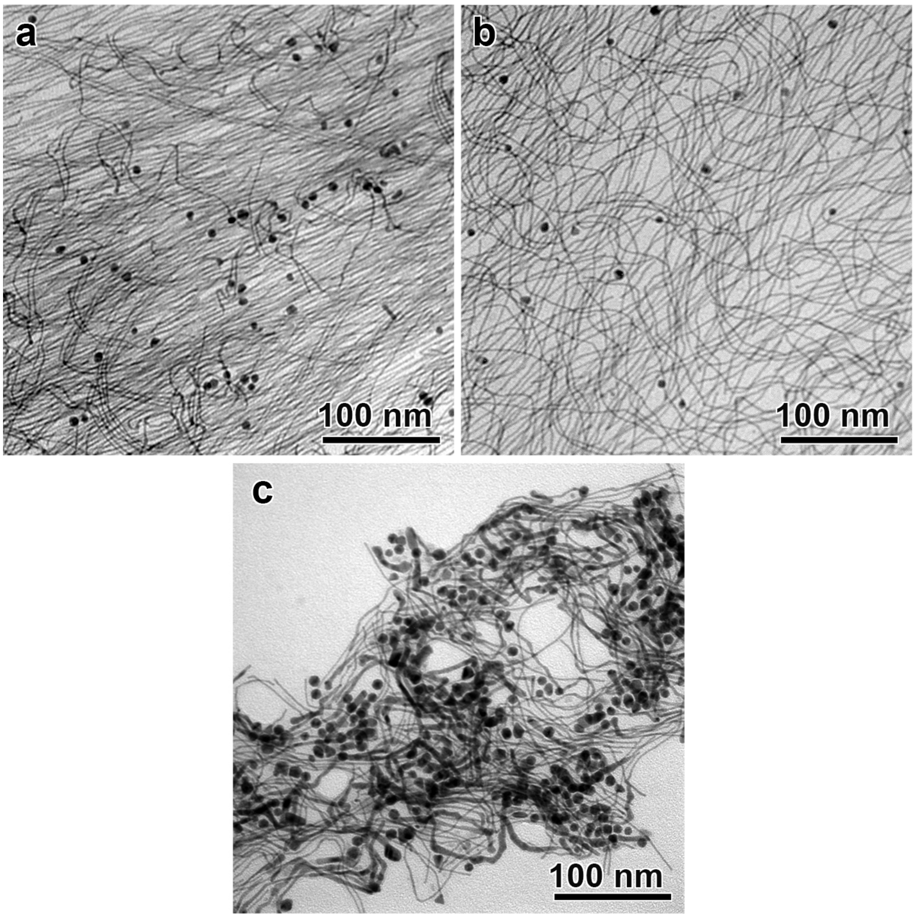

Figure S6. The effect of the Cl$^-$/Ag$^+$ ratio on the formation of the ultrathin Au-Ag alloy nanowires ($HAuCl_4$/$AgNO_3$ = 1.25 in the precursor). In a typical synthesis (see Figure 1), the Cl$^-$/Ag$^+$ ratio (Cl$^-$ from $HAuCl_4$) is 5. The TEM images of the products obtained from different Cl$^-$/Ag$^+$ ratios are shown in (a–c). (a) Cl$^-$/Ag$^+$ = 15; (b) Cl$^-$/Ag$^+$ = 30; (c) Cl$^-$/Ag$^+$ = 50. With increasing Cl$^-$/Ag$^+$ ratios, the reaction time was prolonged to allow a complete reaction, because Cl$^-$ can complex with Ag$^+$ and produce AgCl with a much-decreased reduction potential. The reaction times were 30 min (Cl$^-$/Ag$^+$ = 5, typical synthesis), 1 h (Cl$^-$/Ag$^+$ = 15 and 30), and 5 h (Cl$^-$/Ag$^+$ = 50). It is clear that the ultrathin Au-Ag alloy nanowires could be obtained with a wide range of Cl$^-$/Ag$^+$ (~5–30). When the Cl$^-$/Ag$^+$ ratio was too high (Cl$^-$/Ag$^+$ = 50), a mixture of nanospheres and nanowires was obtained, which could be attributed to the unfavorable reduction kinetics due to the formation of the AgCl precipitates.

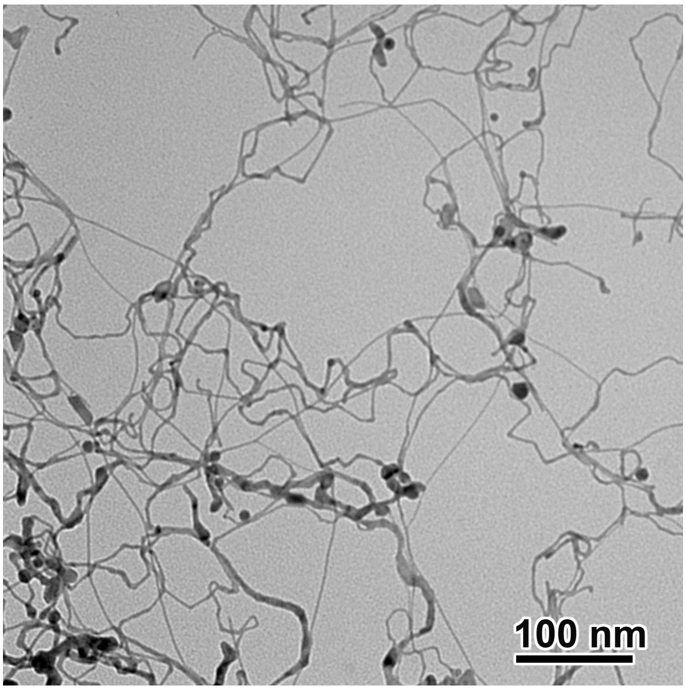

Figure S7. TEM image of the ultrathin Au-Ag alloy nanowires obtained without PVP in a typical synthesis, which rules out the critical role of the PVP in regulating the one-dimensional growth of the nanowires. Large agglomerates exist in the absence of PVP, indicating that PVP is a good dispersant to enhance the colloidal property of the ultrathin Au-Ag alloy nanowires.

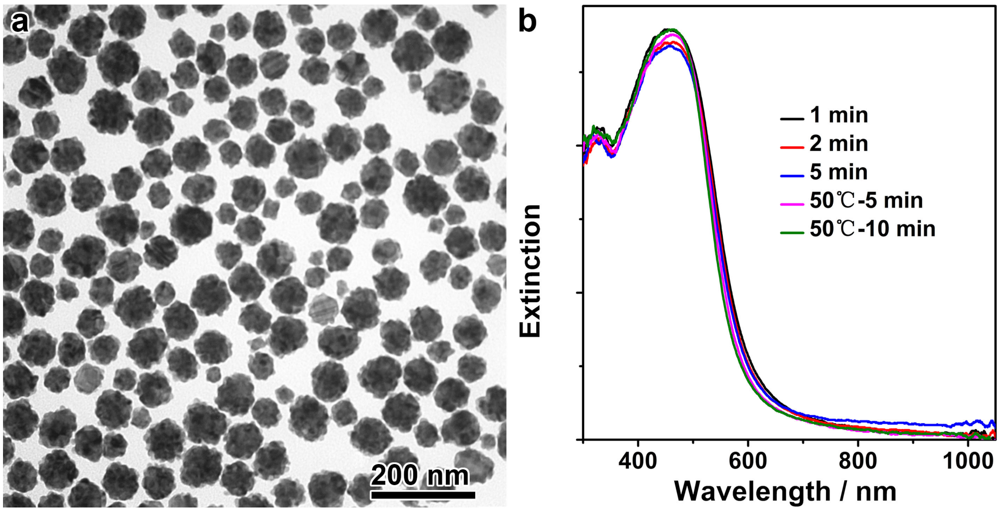

Figure S8. The effect of the DMF in the synthesis of the ultrathin Au-Ag alloy nanowires. (a) TEM image of large nanoparticles obtained from a typical synthesis using H_2O as a solvent in place of the DMF. (b) Time-dependent UV-vis-NIR spectra of the reaction system, indicating that the reaction was almost complete in one minute at room temperature. These results confirm that DMF can significantly reduce the reduction rate of the metal salts to achieve a favorable kinetics for the growth of the nanowires.

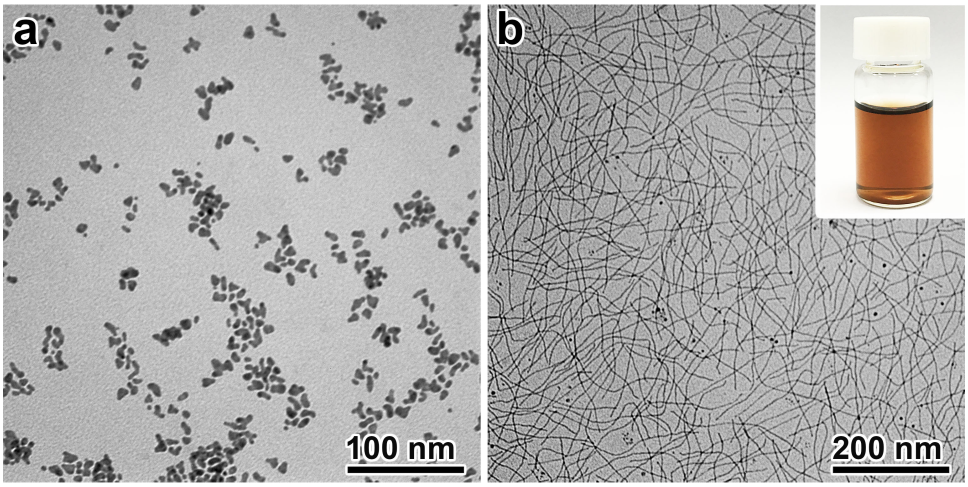

Figure S9. The role of the reaction rate in the synthesis of the ultrathin Au-Ag alloy nanowires. (a–b) TEM image of the product obtained by using ascorbic acid (AA) as the reducing agent with different concentrations of NaOH (A, NaOH/AA = 3:1; B, NaOH/AA = 1:3). The high NaOH/AA ratio leads to a high reduction rate of the metal salts and thus the formation of irregular nanoparticles. A slow reaction rate at a low NaOH/AA ratio leads to ultrathin Au-Ag alloy nanowires of a high quality. It, therefore, confirms that a slow reaction rate is a prerequisite for the successful growth of the ultrathin Au-Ag alloy nanowires.

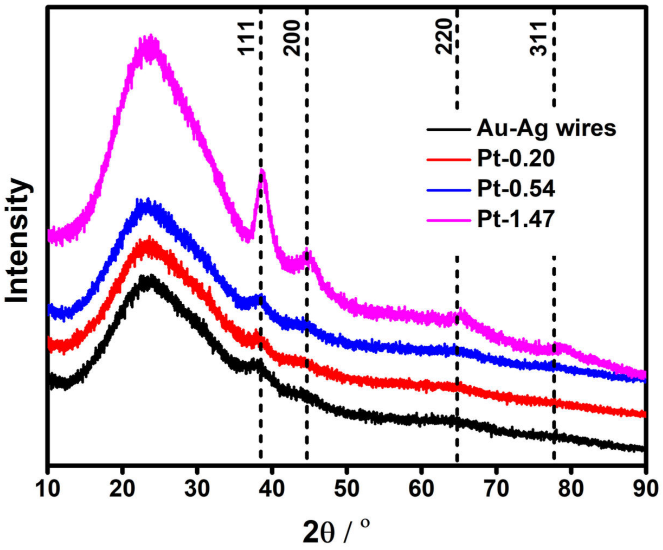

Figure S10. XRD patterns of the ultrathin Au-Ag alloy nanowires and the Au-Ag@Pt core/shell nanowires (Pt-*x*, *x* = 0.20, 0.54, and 1.47). The XRD patterns of the Au-Ag@Pt core/shell nanowires show only a single set of the X-ray reflections, in line with the epitaxial growth of a monolayer or multilayers of Pt in an epitaxial manner. A slight deviation in the position of the X-ray reflections of Pt-1.47 may arise from partial interfacial alloying of Pt with Au and Ag during the crystal growth.

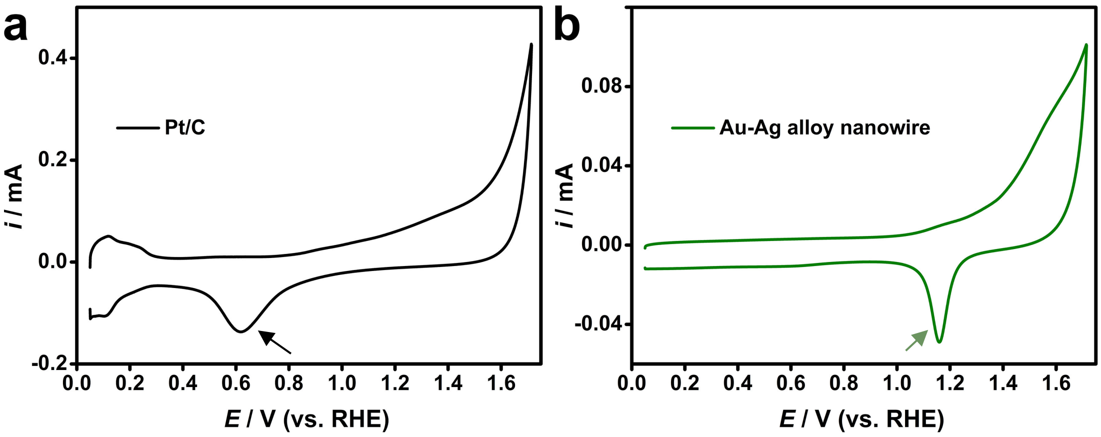

Figure S11. (a–b) CV curves of the Pt/C and the Au-Ag alloy nanowires in N_2-saturated 0.5 M H_2SO_4. In cathodic scans, peaks can be observed at ~ 0.6 (black arrow) and ~ 1.1 V (green arrow) vs. RHE, which corresponds to the reduction of the Pt oxide and Au oxide, respectively.

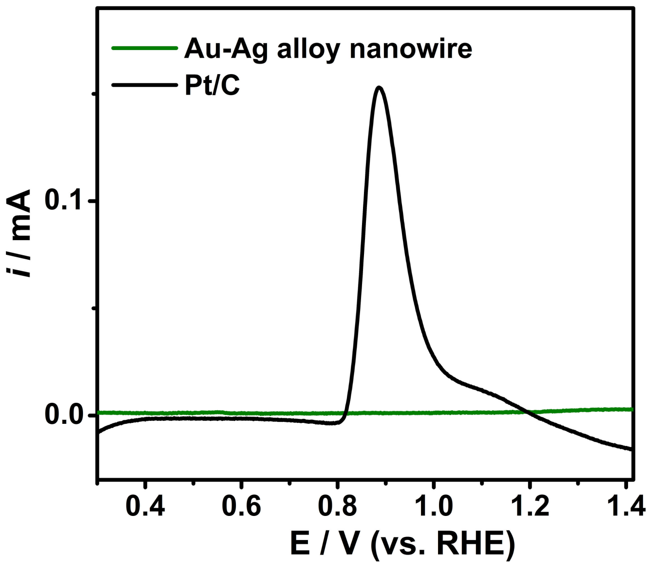

Figure S12. CO stripping of the commercial Pt/C catalyst and the ultrathin Au-Ag alloy nanowires. The ECSA of the Pt/C was determined by the CO stripping to be 102.8 m^2 g^{-1}_{Pt}. No CO stripping peaks were observed with the Au-Ag alloy nanowires.

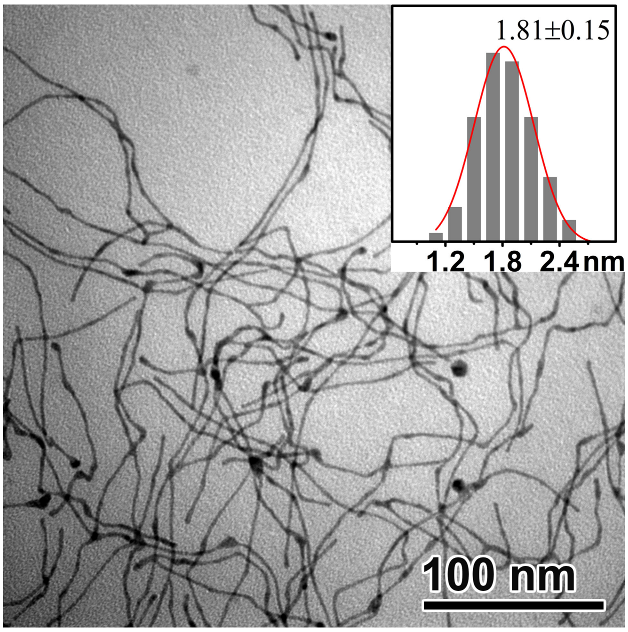

Figure S13. TEM image of the Pt-0.01 catalyst. Inset: Diameter distribution of the nanowires.

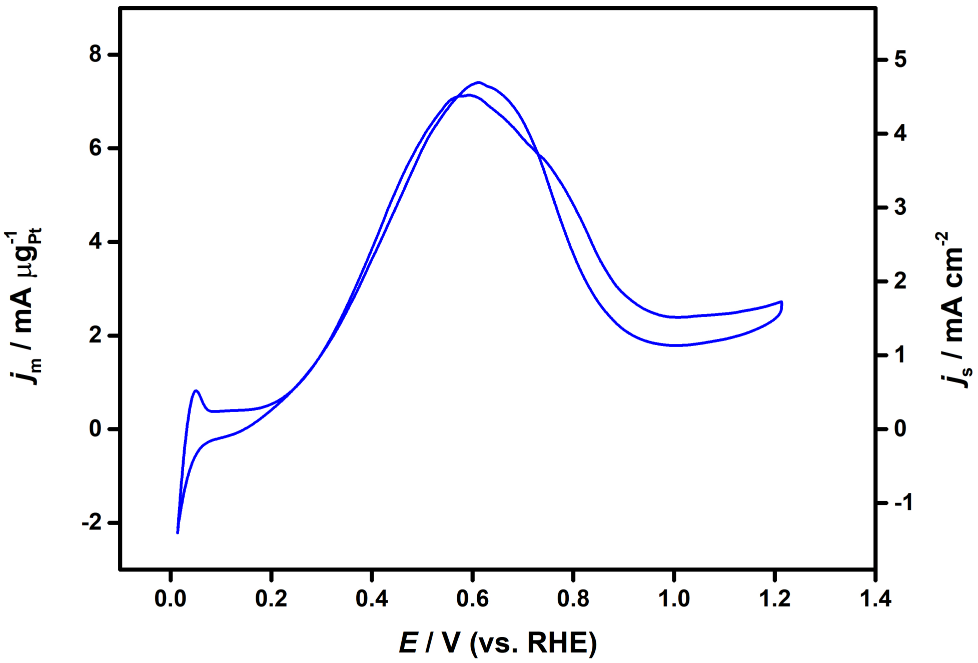

Figure S14. CV curve of the Pt-0.01 catalyst in N_2-saturated HCOOH(0.25 M)/H_2SO_4(0.5 M) at a scan rate of 50 mV s^{-1}. The activities were normalized by the mass and the ECSA of the catalyst, respectively.

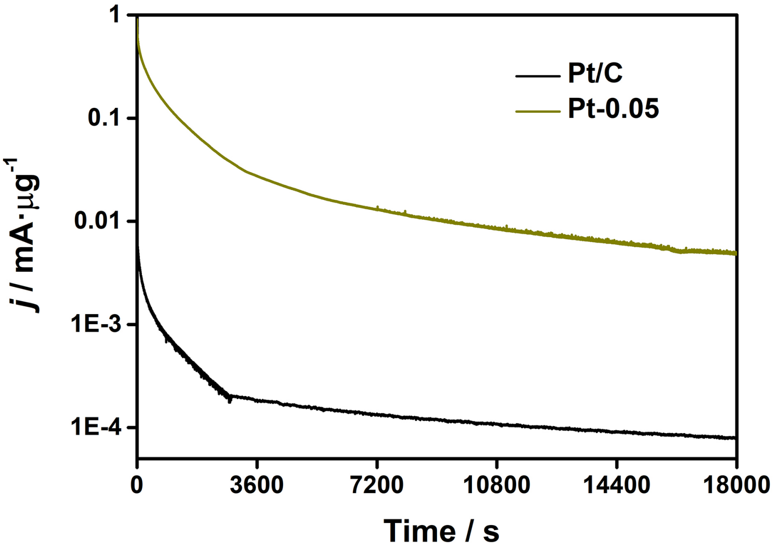

Figure S15. Chronoamperometry curve of the Pt-0.05 and the commercial Pt/C in N_2-saturated HCOOH(0.25 M)/H_2SO_4(0.5 M) at 0.3 V vs. RHE in a long period of 5 h. The Pt-0.05 catalyst showed high catalytic activity in the FAOR. The Pt mass activity of the Pt-0.05 catalyst remained about 2 orders of magnitude higher than that of the commercial Pt/C, even after 5 h. It is worth noting that after 5 h, the nanowires were broken into nanoparticles due to the gradual oxidation of Pt, Au, and Ag at 0.3 V, which may be ascribed to the ultrasmall thickness of the Au-Ag nanowires. Further investigation is still needed to enhance the long-term stability of the catalysts.